

# An algorithm for finding good collective variables for enhanced sampling given limited static and dynamic knowledge

Pratyush Tiwary<sup>1,\*</sup> and B. J. Berne<sup>1,†</sup>

<sup>1</sup>*Department of Chemistry, Columbia University, New York 10027, USA.*

(Dated: February 18, 2022)

In modern day simulations of many-body systems much of the computational complexity is shifted to the identification of slowly changing molecular order parameters called collective variables (CV) or reaction coordinates. A vast array of enhanced sampling methods are based on the identification and biasing of these low-dimensional order parameters, whose fluctuations are important in driving rare events of interest. In this preliminary note, we describe a new algorithm for finding optimal collective variables for use in enhanced sampling biasing methods like “umbrella sampling” and “metadynamics”, and related methods, when limited prior static and dynamic information is known about the system, and a larger set of candidate CVs is specified. The algorithm involves estimating the best combination of these candidate CVs, as quantified by a maximum path entropy estimate of the spectral gap for dynamics viewed as a function of that CV. Through two practical examples, we show how this post-processing procedure can lead to optimization of CV and several orders of magnitude improvement in the convergence of the free energy calculated through metadynamics, essentially giving the ability to extract useful information even from unsuccessful metadynamics runs. A detailed paper will be presented later.

## I. INTRODUCTION

In biomolecular simulations, the following picture typically holds true:

- (a) There are multiple but finitely many stable conformational states in which the system can exist
- (b) There are a large number,  $d$ , of available low-dimensional order parameters and combinations thereof, called collective variables (CV), that can be used to distinguish between these stable states. For a  $N$ -atom system, typically  $1 \ll d \ll N$ , and we refer to this set as  $\{\Theta\}$ .

Given this picture, there are several available techniques [1–4] that can sample the relative probability distributions of the stable states, and also calculate the rate constants for escape from these states [5]. These techniques a subset of the various available order parameters much smaller than  $d$  - typically one to three, whose fluctuations are deemed to be most important for the system or process being studied.

But how does one decide what is an optimal low-dimensional subset or combination of CVs? In other words, which fluctuations matter for the dynamics of the system and which ones don’t? This is a question of general importance, the answer to which decides (a) the speed of convergence of an enhanced sampling simulation or if it will even ever converge within practically useful simulation times, (b) if one can eventually extract rates by biasing along these order parameters. In fact, an identification of these CVs is useful not just for

enhanced sampling in molecular dynamics (MD) simulations but also for distributed computing techniques such as Markov State Models (MSM) [6], allowing one to significantly improve the quality of the constructed kinetic models, and make the best use of the available computing resources. Last but not the least, having an optimal 1 or 2-dimensional CV can also help in the building of Brownian dynamics type models [7]. Indeed, given the importance of this problem, there exists a range of methods that can solve it, at least in theory. In this brief note we wish not to compare against any existing method, and postpone that discussion to the more detailed paper to follow.

Our main hypothesis, which we state without rigorous proof for now, is that the best CV should show the maximum separation of timescales between slow and fast processes [9]. Thus, if the dynamics was to be described solely as a function of this CV, any hidden or missing dynamics in the orthogonal subspace to this CV should rapidly equilibrate relative to the dynamics of this slow CV. This gap in timescales of the slow and fast processes in a system is commonly referred to as the spectral gap, which we define rigorously later in this note. Note that in this work henceforth we refer to the best CV in the singular, without loss of any generalization in the treatment.

The key idea here is to perform enhanced sampling (for eg. metadynamics) with a trial choice of CVs, possibly complemented with short bursts of unbiased MD simulations, and to learn from the limited dynamical and stationary state information gathered to iteratively improve the CVs. The maximum Caliber framework [10–12], which is a dynamical generalization of the hugely popular maximum entropy framework [13], provides just the way to do this.

\* pt2399@columbia.edu

† bb8@columbia.edu

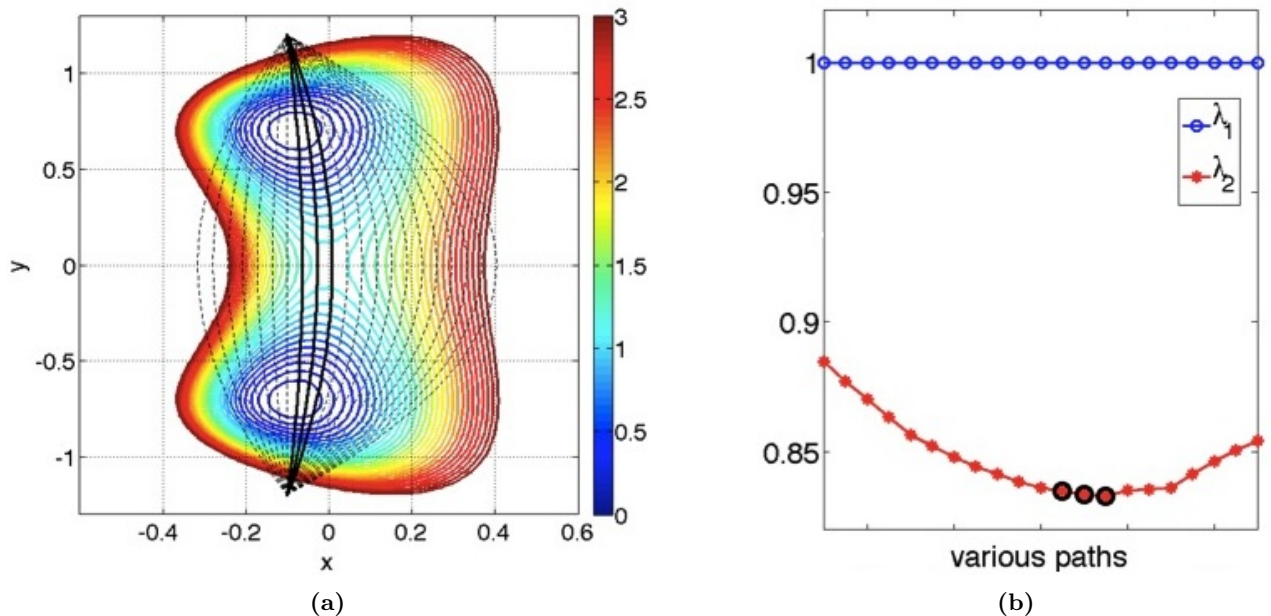


**FIG. 1:** In (a), we provide the De Leon and Berne potential [8] with several candidate path CVs imposed on it (black lines). The parameters and units are the same as the strong coupling case reported in [8]. In (b), the corresponding first and second eigenvalues (i.e. excluding the stationary eigenvalue which is identically 1) are shown for respective dynamics along each of these paths (counting left to right in each figure) is shown, with three possible good paths marked with solid black lines in (a) and black circles in (b).

## II. BRIEF THEORY

Our algorithm aims to address the question of optimizing CVs in a computationally efficient manner. One picks a trial CV given by some  $f\{\Theta\}$ .  $f$  here is function projecting the space  $\{\Theta\}$  onto a 1-dimensional space. For the sake of clarity, we assume that  $f$  is a linear combination of  $\{\Theta\}$ , i.e.  $f = c_1\Theta_1 + c_2\Theta_2 + \dots + c_d\Theta_d$ . The treatment developed here applies to non-linear combinations as well which we show in one of the examples.

We consider the space along this trial CV  $f\{\Theta\}$  to be discretized in grids. Let  $p_n(t)$  denote the instantaneous probability of the system being found in grid  $n$ . Then, for a fixed  $\Delta t$ , we write a master equation:

$$\frac{\Delta p_n(t)}{\Delta t} = \sum_m \omega_{mn} p_m(t) - \sum_n \omega_{nm} p_n(t) \equiv \sum_m \Omega_{nm} p_m(t) \quad (1)$$

where  $\omega_{nm}$  is the rate of transition from grid  $n$  to  $m$  per unit time. The matrix  $\Omega_{nm}$  is the entirety of all these rates. If the dynamics of  $f\{\Theta\}$  is Markovian, then the matrix  $\mathbf{k}$  of transition probabilities given by  $k = \exp(\Omega\Delta t) = \mathbf{I} + \Omega\Delta t$  should not depend on the  $\Delta t$  used in Eq. 1.

Similar to the maximum entropy approach, in the maximum Caliber approach one uses all available stationary state and dynamical information to construct probabilities not of microstates but of *micropaths*. Just like the entropy over states, one now defines an entropy over paths,

which is essentially a path integral. This entropy over paths is defined below for Markovian process:

$$S = -\sum_{ab} p_a k_{ab} \log k_{ab} \quad (2)$$

Path ensemble averages of time-dependent quantities  $A_{ab}$  can now be calculated as [11, 12]

$$\langle A \rangle = \sum_{ab} p_a k_{ab} A_{ab} \quad (3)$$

The path entropy of Eq. 2 incremented by quantities accounting for constraints placed by our knowledge of observables  $\{A_{ab}^n\}$ , and some other constraints such as detailed balance, is collectively called Caliber [11, 12]. The maximum Caliber approach then involves writing and maximizing the Caliber with the end result being that one obtains a relation between the grid-to-grid rates and the stationary probabilities as follows:

$$\omega_{ab} = \frac{1}{\Delta t} \sqrt{\frac{p_b}{p_a}} e^{-\sum_i \rho_i A_{ab}^i} \quad (4)$$

where  $i$  runs over the number of available dynamical pieces of information, and  $\rho_i$  is the Lagrange multiplier for the  $i$ th constraint. For instance, consider when the only observable at hand is the mean number of transitions in  $\Delta t$  over the *entire* network [12], comprising all the grids along a trial CV. In this, the above equation becomes

$$\omega_{ab} = \frac{1}{\Delta t} \sqrt{\frac{p_b}{p_a}} e^{-\rho} \quad (5)$$

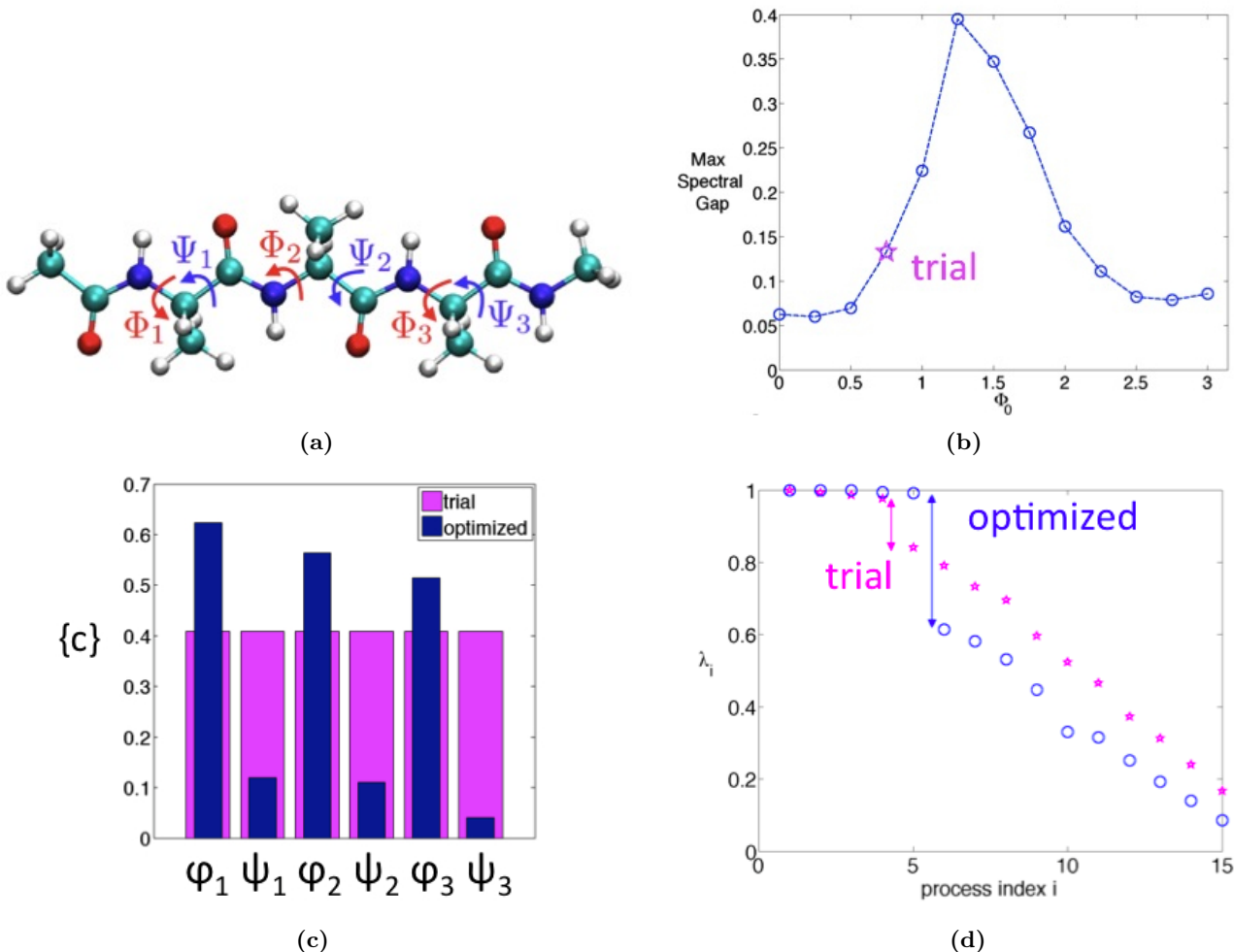


**FIG. 2:** (a) The 3-residue peptide example studied in this work. The six dihedral angles are marked. (b) The output of the simulated annealing algorithm run separately for different  $\Phi_0$  values (blue circles). The starting value with the trial choice of CV is marked with magenta star. (c) The trial (magenta) and optimized (blue) mixing coefficients for the 6 dihedrals. (d) The spectrum of eigenvalues for dynamics projected on the trial (magenta) and optimized (blue) CVs, along with respective spectral gaps.

More information simply introduces additional Lagrange multipliers which can be easily fit to the available unbiased MD or experimental data. The simplest is to define the mean number of transitions not over the entire network but individually over separate basins [12]. Possibly the most accurate is to calculate the local position-dependent diffusivity tensor [14, 15]. There is a huge scope for creativity and improvement here in terms of the dynamic observables to constrain the Caliber, and one could even include experimental observables [16, 17]. One key point to note here is that we are concerned with transitions between neighboring or next-nearest neighboring grids, which means only local rates - no long sampling that requires the crossing of barriers.

We will then look at the spectral gap of the transition probability matrix  $\mathbf{k}$ , which for  $a \neq b$  has  $k_{ab} = \omega_{ab}\Delta t$  and satisfies normalization as described in Ref. [12].

### III. THE ALGORITHM

We are now in a position to describe the actual algorithm. It comprises the following steps in a sequential manner, and can be improved by iterating.

1. Perform metadynamics along a trial CV  $f = c_1\Theta_1 + c_2\Theta_2 + \dots + c_d\Theta_d$  to get a crude estimate of the stationary density. As we pointed out at the end of the last section and also show through examples, what matters is that this estimate be correct locally in the depth of the basin, and not necessarily globally given the short-range nature of terms in Eqs. 4-5.
2. In each of the basins, perform short bursts of unbiased MD runs to sample some dynamical observables  $\{A_{ab}^n\}$ . If Eq. 5 is to be used (which we recommend initially when the trial CV is possibly

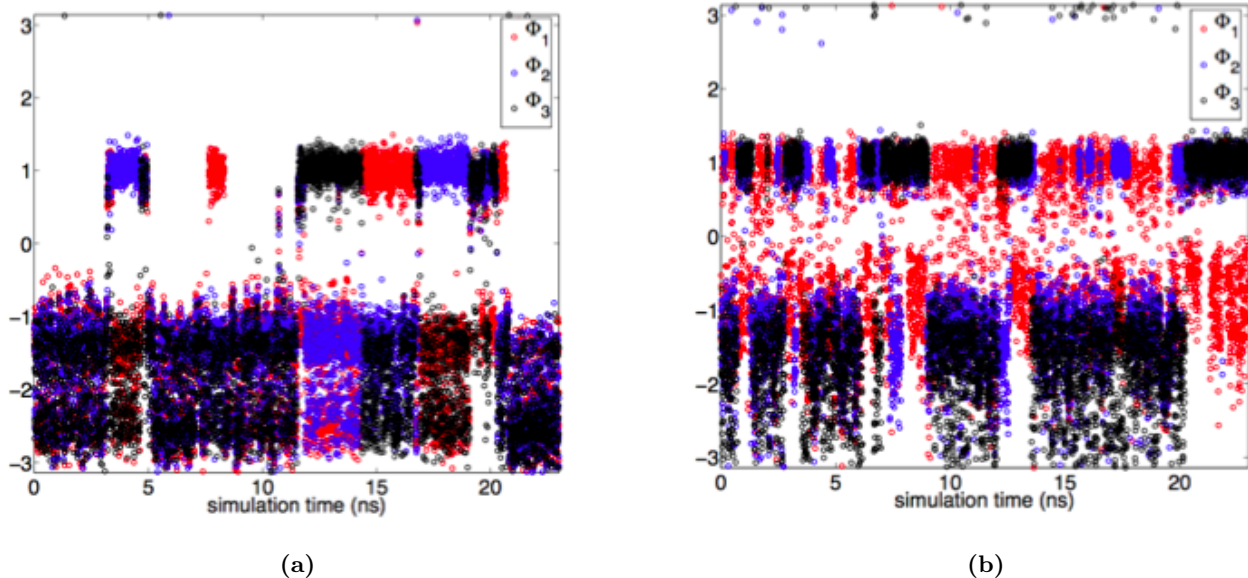


**FIG. 3:** (a) and (b) show trajectories obtained from metadynamics biasing the trial CV and the optimized CV respectively. A very pronounced improvement in the sampling can be seen with the optimized CV.

really poor), then this step can be entirely skipped as it does not matter for the spectral gap in the probability matrix due to normalization.

3. As post-processing, perform optimization (we do simulated annealing) in the space of mixing coefficients  $\{c_1, c_2 \dots c_d\}$  leading to different new CVs, where the objective is to maximize the spectral gap through Eqs. 4-5. The spectral gap is defined for the rate matrix  $\mathbf{k}$  as  $e^{-\lambda_s} - e^{-\lambda_{s+1}}$ , where  $s$  is the number of barriers in the free energy estimate projected on the new CV, that are higher than a user-defined threshold (typically  $\gtrsim k_B T$ ). The reweighting functionality [18] of metadynamics allows projection of free energy estimates on different CVs with minimal computational effort.

The optimization procedure gives the best CV as the one with highest spectral gap, given the information at hand. As in any maximum entropy framework [13], the better is the quality of this information, the more accurate will be the spectral gap. But even with very poor quality information, as we show in the examples, the algorithm still suggests significant improvement in the CV – our objective here is not to get accurate rates, for which we intend to use other methods [5, 22]. Furthermore, Markovianity of the CV can also be checked by repeating step 2 for different time intervals  $\Delta t$  of observation and determining if the spectral gap depends on it.

## IV. ILLUSTRATIVE EXAMPLES

### A. Model 2-d landscape: The De Leon Berne potential

The first example we consider is a model 2-state potential introduced by De Leon and Berne [8]. To sample this landscape at temperature  $k_B T = 0.1$ , we try metadynamics with path CVs, a class of CVs widely used that can capture non-local and non-linear fluctuations (see [23] for details). In Fig. 1 (a) we show the 2-d potential along with several possible path CVs imposed on it. A short trial metadynamics run is performed biasing the y-coordinate, from which the spectral gap is generated for the various paths using Eq. 5 (Fig. 1 (b)). By comparing Fig. 1(a) against Fig. 1(b), it is clear how the path with maximum spectral gap is the lowest energy pathway passing through the saddle point. In this case while this result could have simply been obtained through Nudged Elastic Band type calculations [24] - the point is to use this example to develop intuition for the method. Also note that moving around the best path to others that actually are a bit distant from it, does not lead to much change in the spectral gap. This is consistent with the observation that in several enhanced sampling methods such as metadynamics or umbrella sampling [2, 4, 25], the CV need not be precisely the true reaction coordinate, but should simply have a sufficient overlap with it [23, 26].

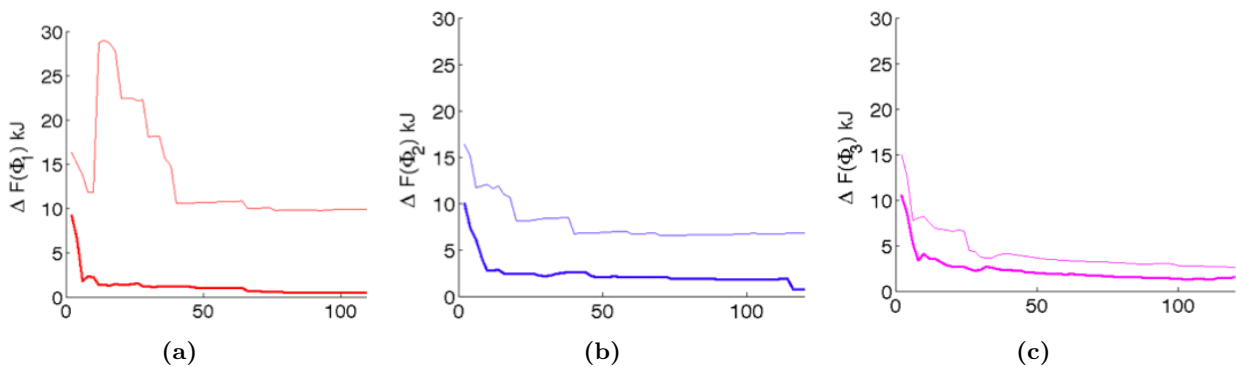


**FIG. 4:** Errors in the 1-d free energies in kJ calculated with respect to reference free energies [19, 20] using the error metric from [21]. Thin and thick lines denote values using the trial and optimized CVs respectively.

### B. 3-residue peptide

Now we move to a more complex system, which has also been considered as a test case for new enhanced sampling methods [19]. This is the 3-residue peptide *Ace - Ala<sub>3</sub> - Nme* (see Fig. 2 (a)), where there are six possibly relevant dihedral torsion angles. Here we ask the question: what is the best possible 1-d linear combination of these six dihedrals that we could bias but still maximally enhance exploration of the 6-d space comprising all the dihedrals?

In this problem, for numerical reasons, we bias a reference cosine defined by  $\cos(\theta - \theta_0)$ , where  $\theta$  is one of the six dihedral angles, and  $\theta_0$  is some reference value whose optimal choice we do not know *a priori*. Through our algorithm we then seek to identify:

- (a) The best choice of mixing coefficients  $\{c\}$  to use in trial CV  $f = c_1\Phi'_1 + c_2\Psi'_1 + c_3\Phi'_2 + c_4\Psi'_2 + c_5\Phi'_3 + c_6\Psi'_3$ , where we keep the euclidean norm of  $\{c\}=1$ , and for any angle  $\theta$  the prime denotes the transformation  $\theta \mapsto 0.5 + \cos(\theta - \theta_0)$ .
- (b) The best choice of  $\Phi_0$ .

We start with the case where all members of  $\{c\}$  are kept the same, and an arbitrary choice of  $\Phi_0 = 0.75$  radians is taken. In Fig. 2 (b-d) respectively, we show how the spectral gap is increased by the simulated annealing procedure, and the corresponding best estimate of  $\{c\}$ . The algorithm suggests the minimal role of the angles  $\Psi_1, \Psi_2, \Psi_3$  as can be seen through their relatively low weights (Fig. 2 (c)). The spectrum of eigenvalues for dynamics projected on the trial (magenta) and optimized (blue) CVs, along with respective spectral gaps is provided in Fig. 2(d). Fig. 3 (a-b) show the metadynamics trajectories for the three dihedral angles  $\Phi_1, \Phi_2, \Phi_3$  with the trial and the optimized CVs respectively. A very pronounced improvement in the sampling can be seen. Fig. 4 (a-c) shows the rate of convergence of the error of the estimated free energy [18] with respect to reference values from other approaches

[19]. The error metric is the same as in [21], and is calculated for all points within 25 kJ of the global minimum in the respective 1-d free energy. The behavior is robust with respect to the choice of this threshold value. As can be seen, the optimized CV, even though it was obtained on the basis of a very poorly converged and short (20 ns) metadynamics run, and in this case through the simple use of Eq. 5, leads to several orders of magnitudes improvement in the rate at which the three free energies converge.

## V. CONCLUSIONS

To conclude, we have introduced a new approach for the improving the choice of collective variables to be biased in enhanced sampling in complex systems. This is accomplished through the use of maximum Caliber based spectral gap estimates. The algorithm is iterative in spirit, but even with 1 iteration for a small peptide, we found very significant improvement in finding the best 1-d collective variable from possible 6 with no *ad hoc* or intuition based tuning. Future work will use this algorithm to consider a range of problems, especially in the context of protein-ligand unbinding. For instance, the displacement of water molecules and protein flexibility are often slowly varying order parameters in unbinding [26–29], but do we really need to bias one or both of these for the purpose of sampling? Another question to be considered in future work will be using these optimized CVs to obtain reliable dynamical information from metadynamics [5, 22] such as the off-rate for ligand unbinding. A more detailed paper will follow with further detailed theory and results.

We would like to thank Purushottam Dixit for helpful discussions regarding Caliber, Omar Valsson for providing system set-up and reference free energies for the peptide and Jed Brown for originally suggesting a spectral gap approach.

- 
- [1] P. G. Bolhuis, D. Chandler, C. Dellago, and P. L. Geissler, *Ann. Rev. Phys. Chem.* **53**, 291 (2002).
- [2] G. M. Torrie and J. P. Valleau, *J. Comp. Phys.* **23**, 187 (1977).
- [3] E. Carter, G. Ciccotti, J. T. Hynes, and R. Kapral, *Chem. Phys. Lett.* **156**, 472 (1989).
- [4] A. Laio and M. Parrinello, *Proc. Natl. Acad. Sci.* **99**, 12562 (2002).
- [5] P. Tiwary and M. Parrinello, *Phys. Rev. Lett.* **111**, 230602 (2013).
- [6] G. Pérez-Hernández, F. Paul, T. Giorgino, G. De Fabritiis, and F. Noé, *J. Chem. Phys.* **139**, 015102 (2013).
- [7] J. A. Morrone, J. Li, and B. J. Berne, *J. Phys. Chem. B* **116**, 378 (2011).
- [8] N. De Leon and B. Berne, *J. Chem. Phys.* **75**, 3495 (1981).
- [9] R. R. Coifman, I. G. Kevrekidis, S. Lafon, M. Maggioni, and B. Nadler, *Mult. Mod. Sim.* **7**, 842 (2008).
- [10] E. T. Jaynes, *Ann. Rev. Phys. Chem.* **31**, 579 (1980).
- [11] S. Pressé, K. Ghosh, J. Lee, and K. A. Dill, *Rev. Mod. Phys.* **85**, 1115 (2013).
- [12] P. D. Dixit, A. Jain, G. Stock, and K. Dill, arXiv preprint arXiv:1504.01277 (2015).
- [13] E. T. Jaynes, *Phys. Rev.* **106**, 620 (1957).
- [14] G. Hummer, *N. Jour. Phys.* **7**, 34 (2005).
- [15] F. Marinelli, F. Pietrucci, A. Laio, and S. Piana, *PLoS Comput. Biol* **5**, e1000452 (2009).
- [16] B. Berne, P. Pechukas, and G. Harp, *J. Chem. Phys.* **49**, 3125 (1968).
- [17] D. Granata, C. Camilloni, M. Vendruscolo, and A. Laio, *Proc. Natl. Acad. Sci.* **110**, 6817 (2013).
- [18] P. Tiwary and M. Parrinello, *J. Phys. Chem. B* **119**, 736 (2015).
- [19] O. Valsson and M. Parrinello, *Phys. Rev. Lett.* **113**, 090601 (2014).
- [20] O. Valsson and M. Parrinello, *J. Chem. Theor. Comp.* (2015).
- [21] D. Branduardi, G. Bussi, and M. Parrinello, *J. Chem. Theor. Comp.* **8**, 2247 (2012).
- [22] M. Salvalaglio, P. Tiwary, and M. Parrinello, *J. Chem. Theor. Comp.* **10**, 1420 (2014).
- [23] D. Branduardi, F. L. Gervasio, and M. Parrinello, *J. Chem. Phys.* **126**, 054103 (2007).
- [24] G. Henkelman, B. P. Uberuaga, and H. Jónsson, *J. Chem. Phys.* **113**, 9901 (2000).
- [25] A. Barducci, G. Bussi, and M. Parrinello, *Phys. Rev. Lett.* **100**, 020603 (2008).
- [26] P. Tiwary, V. Limongelli, M. Salvalaglio, and M. Parrinello, *Proc. Natl. Acad. Sci.* **112**, E386 (2015).
- [27] J. E. Ladbury, *Chem. Bio.* **3**, 973 (1996).
- [28] B. J. Berne, J. D. Weeks, and R. Zhou, *Annual review of physical chemistry* **60**, 85 (2009).
- [29] P. Tiwary, J. Mondal, J. A. Morrone, and B. J. Berne, *Proc. Natl. Acad. Sci.* (2015), 10.1073/pnas.1516652112.